Transcriptome analysis of the inhibitory effect of cycloleucine on myogenesis

Zhijun Wang,[*,†] Danfeng Cai,[*,†] Kan Li,[*,†] Xing Ju,[*,†] and Qinghua Nie[*,†,1]

[*]*Department of Animal Genetics, Breeding and Reproduction, College of Animal Science, South China Agricultural University, Guangzhou 510642, China; and* [†]*National-Local Joint Engineering Research Center for Livestock Breeding, Guangdong Provincial Key Lab of Agro-Animal Genomics and Molecular Breeding, and Key Laboratory of Chicken Genetics, Breeding and Reproduction, Ministry of Agriculture, Guangzhou 510642, China*

ABSTRACT N6-Methyladenosine (**m^{6}A**) has been reported to involve and play an important role in various biological activities but seldom in poultry myogenesis. Cycloleucine usually functions as a nucleic acid methylation inhibitor, the inhibition efficiency of cycloleucine at the m^{6}A level and corresponding dynamic changes of poultry muscle cells remain unknown. In this study, we aim to find out the effect of cycloleucine on the total N6-Methyladenosine level and its molecular mechanism for regulating myogenesis. A total of 745 differentially expressed genes (**DEG**s) were obtained by 10 mM, 20 mM, and 30 mM of cycloleucine treatment compared with 0 mM treatment. DEGs in 10 mM cycloleucine were significantly enriched in the biological process of skeletal muscle and satellite cell proliferation and differentiation, DEGs in 20 and 30 mM cycloleucine were enriched in some metabolic and biosynthetic processes. The trend analysis showed that 85% of all DEGs were significantly clustered into 4 files, among them 59% DEGs were dose-dependent and 26% were dose-independent, 52% DEGs were in downtrend and 33% DEGs were in uptrend. Also, the cycloleucine treatment could trigger cell cycle arrest in the G1 phase and depress myoblast cell proliferation and inhibit myotube formation. In conclusion, cycloleucine could continuously reduce the m^{6}A level of myoblast cells, depress myoblast cell proliferation and inhibit myotube formation.

Key words: cycloleucine, N6-Methyladenosine, myogenesis, mRNA-Seq, chicken

2022 Poultry Science 101:102219
https://doi.org/10.1016/j.psj.2022.102219

BACKGROUND

Cycloleucine (1-aminocyclopentane-1-carboxylic acid) is a nonmetabolizable amino acid, that could function as a nucleic acid methylation inhibitor, and reduce the S-adenosyl methionine level by participating in the synthesis of S-adenosyl-L-methionine (methyl donor) and inhibit ATP enzyme (L-methionine S-adenosyl transferase) activity and the methionine adenosyl transferase reaction (Lombardini et al., 1970a; Coulter et al., 1974; Caboche and Bachellerie, 1977; Amor and Webb, 1987). Studies have shown that different concentrations of cycloleucine can inhibit the methylation level of RNA in different species (Dimock and Stolzfus, 1978; Chen et al., 2019).

N6-Methyladenosine (**m^{6}A**) is an RNA modification that occurs on adenosine and is the first reversible and most common RNA chemical modification ever found (Jia et al., 2011; Fu et al., 2014; Lee et al., 2014). It has been reported that m^{6}A is wildly involved and played an important role in various biological activities such as embryonic cell differentiation (Wang et al., 2014), embryonic fibroblasts' circadian clock (Fustin et al., 2013), yeast meiosis (Schwartz et al., 2013), mouse spermatogenesis (Zheng et al., 2013), and so on. Previously study showed that METTL3 (an m^{6}A methyltransferase) could regulate muscle stem cell/myoblast state transition (Gheller et al., 2020), and the knockdown of METTL14 (an m^{6}A methyltransferase) in C2C12 myoblast cells could inhibit the differentiation and promote the proliferation of C2C12 myoblast cells (Zhang et al., 2020). The silencing of FTO (an m^{6}A demethylase) could lead to impaired differentiation and fusion of C2C12 myoblast cells (Wang et al., 2017). These results indicate that m^{6}A is directly related to muscle growth and development. So far most of the m^{6}A-related research was in mammals or plants but rarely reported in poultry, especially chicken myogenesis.

Myogenesis is a complex process that contains mainly 4 stages: somite differentiation into myogenic precursors, myogenic precursor proliferates and differentiates

Received May 6, 2022.
Accepted September 29, 2022.

[1]Corresponding author: nqinghua@scau.edu.cn

into my-oblasts, myoblast proliferation, determination, differentiation, and fusion into myotube, myotubes fusion into myofibers (Tajbakhsh, 2009; Feng et al., 2011; Bentzinger et al., 2012; Luo et al., 2013;). The proliferation and differentiation of myoblasts could determine the number of myofibers as well as meat production after birth (Li et al., 2021). There are numerous genes mainly myogenic regulatory factors (**MRF**s) could regulate skeletal muscle differentiation, especially the MyoD family members (MyoD, Myf5, MyoG, MRF4) (Sartorelli and Caretti, 2005; Ferri et al., 2009). Myomarker (Millay et al., 2013) and c-Myc (Luo et al., 2019) are other 2 important genes that were reported to regulate myoblast fusion and muscle formation.

Although cycloleucine was known as a methylation inhibitor, its RNA methylation inhibition effect in poultry myoblast cells has not been verified, as well as the influence of myoblast cells after the reduction of RNA methylation level. Here in this study, we treated chicken primary myoblasts with different concentrations of cycloleucine to detect the changes in m^6A levels and RNA transcription levels as well as its effects on myogenesis.

MATERIALS AND METHODS

Chicken Primary Cell Isolation and Culture

The chicken primary myoblast isolation protocol were handled in compliance and approved by the Animal Care Committee of South China Agricultural University (Guangzhou, China) with approval number SCAU#2020C030.

Each chicken primary myoblast isolation procedure took 10 embryos at the age of 11 d, separated the leg muscle, and cut them into pieces. Digest the muscle tissues for 10 min with 0.25% trypsin (Gibco, Carlsbad, CA) and neutralization with complete growth medium (**GM**) (RPMI-1640 medium (Gibco) with 20% fetal bovine serum (Gibco) and 0.5% penicillin/streptomycin (Gibco)) and the slurry then pass twice through 70- and 40-μm filters and centrifugation at 500 × g for 5 min. Fibroblasts were removed by using the differential velocity adherent method (2 times, 40 min each), and the supernatant was kept and seeded in 100 mm dishes and placed in the incubator for chicken primary myoblast cell culture for 48 h. For proliferation assay, the primary myoblast cells were digested with trypsin and seeded at a density of 2×10^4 cells/cm^2 on 12 well culture plates with a growth medium (**GM**) and treated with cycloleucine after 24 h.

Cycloleucine Treatment

Cycloleucine (MedChemExpress, Monmouth Junction, NJ) was diluted in a growth medium or differentiation medium and passed through a 0.22 μm filter. Different concentrations of cycloleucine (0, 10, 20, 30 mM) were added into 12-well plates (3 wells per treatment) three times to treat cells in the proliferation and differentiation phase for 24 h.

RNA Extraction, Library Construction and mRNA Sequencing (mRNA-Seq)

Total RNA of myoblast cells treated with cycloleucine (0, 10, 20, 30 mM) was extracted using a Trizol reagent kit (Invitrogen, Waltham, MA), and each group named Cyc_0, Cyc_10, Cyc_20, Cyc_30. Total RNA was enriched by Oligo(dT) beats and fragmented into short fragments and reversely transcribed into cDNA by using NEBNext Ultra RNA Library Prep Kit for Illumina (NEB#7530). The purified double-stranded cDNA fragments were end repaired, A base added, and ligated to Illumina sequencing adapters. Ligated fragments were subjected to size selection by agarose gel electrophoresis and PCR amplified. The resulting cDNA library was sequenced on an Illumina Novaseq6000 with paired end 100 bp reads by Gene Denovo Biotechnology Co. (Guangzhou, China).

Bioinformatic analysis was performed using Omicsmart, a dynamic real-time interactive online platform for data analysis (http://www.omicsmart.com).

Trend analysis: gene expression pattern analysis is used to cluster genes of similar expression patterns for multiple samples. To examine the expression pattern of Differentially Expressed Genes (**DEGs**), the expression data of each sample (in the order of treatment) were clustered by Short Time-series Expression Miner software (**STEM**) (Ernst J and Bar-Joseph, 2006). The parameters were set as follows:

1) Maximum unit change in model profiles between time points is 1;
2) Maximum output profiles number is 20 (similar profiles will be merged);
3) Minimum ratio of the fold change of DEGs is 2.0.

The clustered profiles with P-value ≤0.05 were considered as significant profiles. Then the DEGs in all or each profile were subjected to Gene Ontology (GO) and KEGG pathway enrichment analysis. Through the hypothesis test of the P-value calculation and FDR correction (Glickman et al., 2014), the GO terms or Pathways with Q value ≤0.05 were defined as significant enriched GO terms or pathways.

All the sequence data have been deposited in CNCB (China National Center for Bioinformation) Genome Sequence Archive (GSA, https://ngdc.cncb.ac.cn/gsub/) and are accessible through GSA series accession number CRA006597: https://ngdc.cncb.ac.cn/gsa/s/EBPE791w.

cDNA Synthesis and Quantitative Real-Time PCR

cDNA synthesis was carried out using a HiScript II Q RT SuperMix for qPCR (+ gDNA wiper) (Vazyme, China). Quantitative Real-Time PCR (**qRT-PCR**) reactions were carried out in a QuantStudio 5 Real-Time PCR Systems (Thermo Fisher) with iTaq Universal SYBR Green Supermix (Bio-Rad, Hercules, CA).

The primers used for qRT-PCR were listed in Supplementary Table 1.

RNA Dot Blot and Methylene Blue

Total RNA (2 μg) was denatured at 95°C for 3 min and chilled on ice immediately, dropped RNA onto the nylon membrane (Beyotime, China), and crosslinked RNA to the membrane with UV light: 125 mJoule/cm^2 at 254 nm for 60 s. The membrane was washed in TBST for 5 min and blocked in 5% silk milk in TBST for 1 h and incubated overnight with N6-Methyladenosine primary antibody (1:500, #56593, Cell Signaling Technology). HRP conjugated goat-anti rabbit IgG (1:10000, Abbkine) was used as secondary antibodies and incubated for 1 h. Washed the membrane in TBST 3 times for 10 min and captured with a Licor Odyssey (Licor, Lincoln, NE). Methylene blue solution (0.1%) was used for 30 min staining after RNA was crosslinked to the membrane and washed with TBST 3 times for 10 min to measure the total nucleic acid level.

Proliferation Assay

EdU assay: EdU (5-Ethynyl-2′-Deoxyuridine) assay was performed with a C10310 EdU Apollo In Vitro Imaging Kit (Ribobio, Guangzhou, China) after myoblasts were incubated in 50 μM 5-ethynyl-2′-deoxyuridine for 2 h after 22 h cycloleucine treatment. All images were captured with a Leica DMi8 fluorescent microscope (Leica, Wetzlar, Germany) in 200X with 6 random fields in 3 wells per group, the proliferation rate = (EdU positive cells)/ (total Hoechst 33342 stained cells)

Cell cycle analysis: myoblasts were harvested after 24 h cycloleucine treatment and fixed in 70% ethanol overnight at -20°C. Then the cells were incubated with 50 μg/mL propidium iodide (Sigma, St. Louis, MO), 10 μg/mL RNase A (Takara, Japan), and 0.2% Triton X-100 (Sigma) for 30 min at 4°C. Cell cycle analysis was performed with a BD AccuriC6 flow cytometer (BD Biosciences, Franklin Lakes, NJ) and FlowJo (v7.6) software (Treestar Incorporated, Woodburn, OR).

CCK-8 Assay: CCK-8 (Cell Counting Kit 8) assay was performed in a 96-well plate with 10 μL CCK solutions and incubated for 1 h in the cell incubator after 23 h, 35 h, and 47 h cycloleucine treatment. The absorbance was measured in a Fluorescence/Multi-Detection Microplate Reader (BioTek, Winooski, VT) at the wavelength of 450 nm.

Differentiation Assay

The chicken primary myoblast cells were digested with trypsin and seeded at a density of 2×10^4 cells/cm^2 on 12 well culture plates with a growth medium (GM). The medium was replaced with differentiation medium (DM) (RPMI-1640 medium with 5% horse serum and 0.5% penicillin/streptomycin) after 12 h to induce myoblasts differentiation and we defined this day as day 1 (**D1**). The cycloleucine was added on day 2, and the cells were fixed and stained after 24 h, which was cycloleucine treated on day 2 and stained on day 3. Chicken primary myoblasts were fixed with 4% formaldehyde and blocked in 0.2% Triton-X 100 and 5% horse serum with PBS for 30 min, and incubated overnight with MF20 (1:100, Developmental Studies Hybridoma Bank) primary antibody, removed the primary antibody, and washed with PBS for 3 times and incubated with goat anti-mouse IgG (H+L)-Dylight 594 (1:200, BS10027; Bioworld, Minneapolis, MN) and Hoechst 33342 (1mg /mL, H1399, Invitrogen) for 1 h. Rinsed with PBS 3 times for 5 min and leave the cultures in PBS for imaging. All images were captured with a Leica DMi8 fluorescent microscope (Leica, Germany) in 200X with 6 random fields in 3 wells per treatment, and the percentage of myotube area were calculated by ImageJ software (National Institutes of Health, Bethesda, MD).

Statistical Analysis

The relative expression of all detected RNA at differentiation concentrations was compared with 0 mM and calculated by using the 2(-Delta Delta C(T)) method (Livak and Schmittgen, 2001). The statistically significant difference between 0 mM and other concentrations were tested by an independent sample t-test. All results were presented as mean ± S.E.M with at least three replications. We considered $P < 0.05$ to be statistically significant. $^*P < 0.05$; $^{**}P < 0.01$; $^{***}P < 0.001$.

RESULTS

Summary of Transcriptome Data and Differentially Expressed Genes (DEGs)

A total of 12 samples from the myoblast cells with 3 replications per cycloleucine treatments (0, 10, 20, 30 mM) were collected for mRNA-Seq. All raw data were submitted to the CNCB GSA database (accession number CRA006597). In the mRNA-Seq results, we acquired at least 41.29 million clean reads and 6.21 billion clean bases for each sample. The clean reads were mapped to chicken GRCg6a (Ensembl_release100) and detected a total of 17,355 genes with 16,666 known genes and 689 novel genes (Supplementary Table 2). The Principal Component Analysis (PCA) showed that samples from different treatments had their own aggregation distribution while samples from the same treatment appeared similar (Figure 1A). The standard of differentially expressed genes (DEGs) was set as | (Fold change) | ≥ 2 and FDR < 0.05. Compared to the Cyc_0 control group, other treatment groups caused a total of 745 DEGs, among them 106 genes were commonly differentially expressed in three treatment groups, and there were also overlapping DEGs among different treatment groups (Figure 1C). The number of DEGs increases with the increase of concentration, 124 DEGs in Cyc_10, 384 DEGs in Cyc_20, and 676 DEGs in Cyc_30

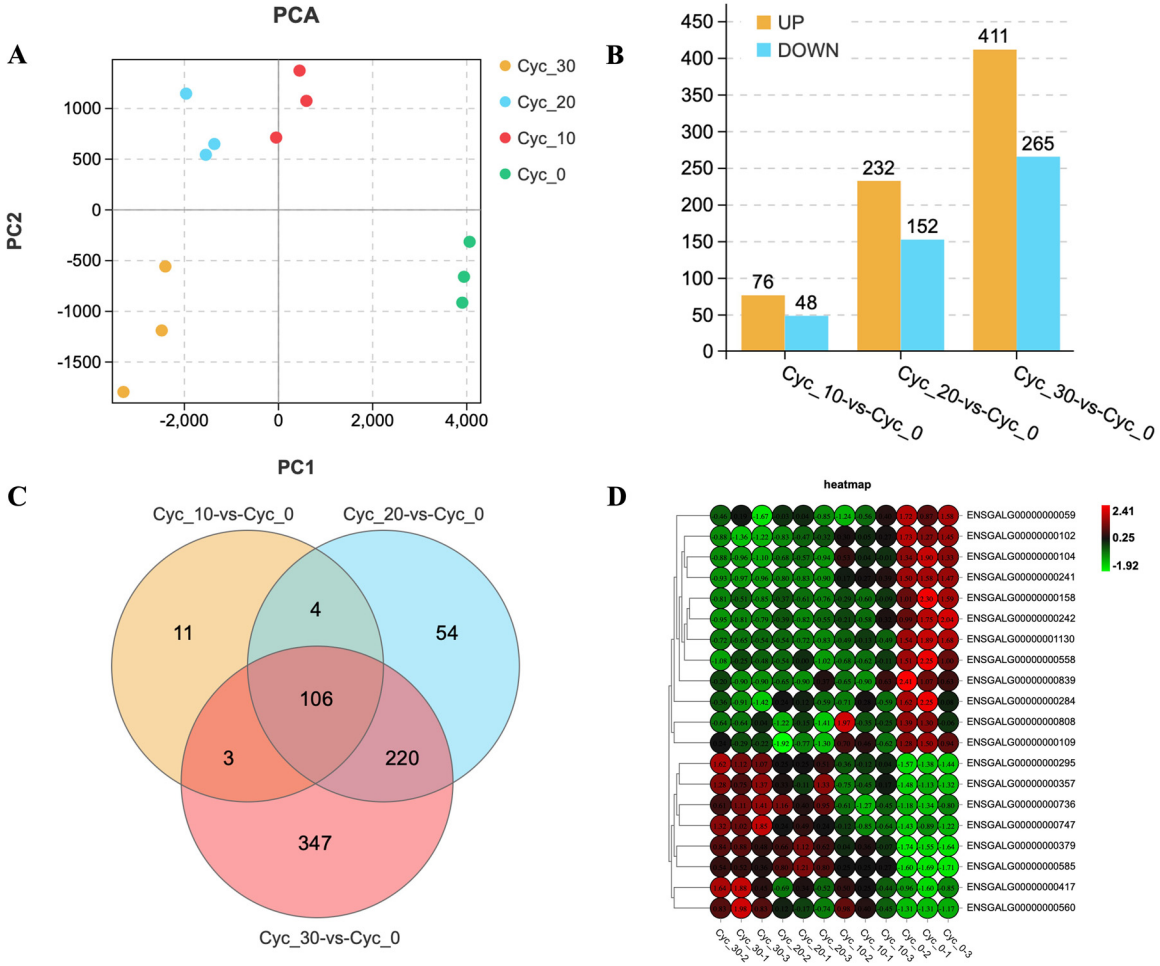

Figure 1. Overview of mRNA sequencing. (A) Principal component analysis for each mRNA-Seq sample. (B) The number of differentially up and down expressed genes in each group. (C) Venn Diagram shows common and unique DEGs between groups. (D) Heatmap for 20 DEGs, the expression went higher when the color become redder and lower in green.

(Figure 1B). The heatmap of 20 DEGs (Supplementary Table 3) showed that the gene expression pattern was different between groups while similar intra-group (Figure 1D).

GO and KEGG Pathway Analysis for Cycloleucine Treatments

The gene ontology (**GO**) functional enrichment of DEGs between three treatment groups was performed together and consistent with our expectation, and GO functional enrichment analysis showed that the enrichment terms of the three experimental groups were similar and the DEGs number was raised with the increase of concentration (Supplementary Figure 1), suggesting a dose-dependent manner of cycloleucine treatment. Specifically, GO functional annotation were divided into Biological Process, Molecular Function, and Cellular Component three section, altogether those DEGs were classified and enriched into 55 terms, 27 terms for biological process, 11 terms for molecular function, and 17 terms for cellular component (Supplementary Figure 1, Supplementary Table 4). The top 20 significant enriched GO terms in Cyc_10 were mainly on muscle and satellite cell proliferation and differentiation and development (Figure 2A, Supplementary Table 5). While in Cyc_20 and Cyc_30, the GO enriched terms went to sterol, steroid, cholesterol, isoprenoid, secondary alcohol, and lipid metabolic and biosynthetic process (Figure 2B, C, Supplementary Tables 6 and 7). The KEGG (Kyoto Encyclopedia of Genes and Genomes) pathway analysis for all groups was divided into six parts as shown in Supplementary Figure 2, as the concentration increased, the genes enriched in each pathway raised. The pathways Cyc_10 enriched were mainly in the serotonergic synapse, neuroactive ligand-receptor interaction, pathways in cancer, FoxO, and TGF-beta signaling pathway, and so on (Figure 3A, Supplementary Table 8). The significantly enriched pathways of the Cyc_20 treatment group were focused on steroid biosynthesis, terpenoid backbone biosynthesis, and metabolic pathways (Figure 3B, Supplementary Table 9). The significantly enriched pathways of Cyc_30 were more enriched in DNA replication than the Cyc_20 group (Figure 3C, Supplementary Table 10).

Gene Expression Pattern Analysis for Cycloleucine Treatments

To confirm whether cycloleucine treated myoblast cells were dose-dependent, we performed a trend

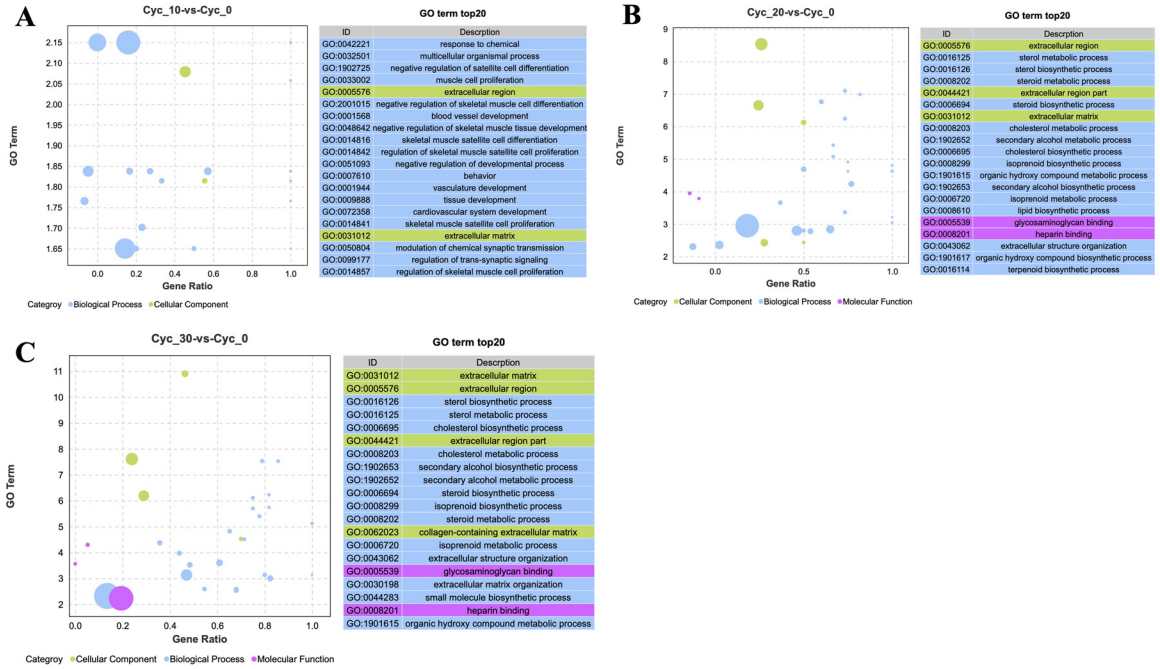

Figure 2. GO functional enrichment analysis. (A−C) GO functional enrichment analysis of DEGs in Cyc_10 (A), Cyc_20 (B), and Cyc_30 (C). X-axis: Proportion of the difference between the number of up-regulated genes and the number of down-regulated genes in the total differential genes. Y-axis: - log10(Qvalue). The size of the bubble indicated the number of genes enriched in current term.

analysis for all 745 DEGs, altogether there could have 20 expression profiles for 4 groups and our DEGs covered 17 profiles (Figure 4A, Supplementary Table 11) but only 4 profiles (profile 0, 19, 2, 17) were clustered significant (Figure 4B, Supplementary Table 12). The genes in these 4 profiles were almost 85% of total DEGs, 59% DEGs were dose-dependent (profile 0 and profile 19) and 26% were dose-independent (profile 2 and profile 17), 52% DEGs were in downtrend (profile 0 and profile 2), 33% DEGs were in uptrend (profile 17 and profile 19). We performed GO and KEGG analysis for these 4 profiles and the GO analysis for profile 0 and 19 have similar terms (Figure 4C, D, Supplementary Tables 13 and 14), but the KEGG pathway analysis showed a little bit difference, genes in profile 0 significantly enriched in metabolic pathways (Figure 4E, Supplementary Table 15), DNA replication, fatty acid metabolism, etc. while profile 19 only significantly enriched in ABC transporters (Figure 4F, Supplementary Table 16). The GO and KEGG analysis for profile 2 and 17 were shown in Supplementary Figure 3.

Cycloleucine Depresses Myoblast Cells Proliferation

Previously study showed that cycloleucine could function as a nucleic acid methylation inhibitor, so we performed an RNA dot blot using the N6-Methyladenosine (m^6A) primary antibody to detect the influence of cycloleucine on N6-Methyladenosine. With the same amount of RNA, the m^6A level continues to decrease with the increase of cycloleucine concentration (Figure 5A-B) in myoblast cells. The above

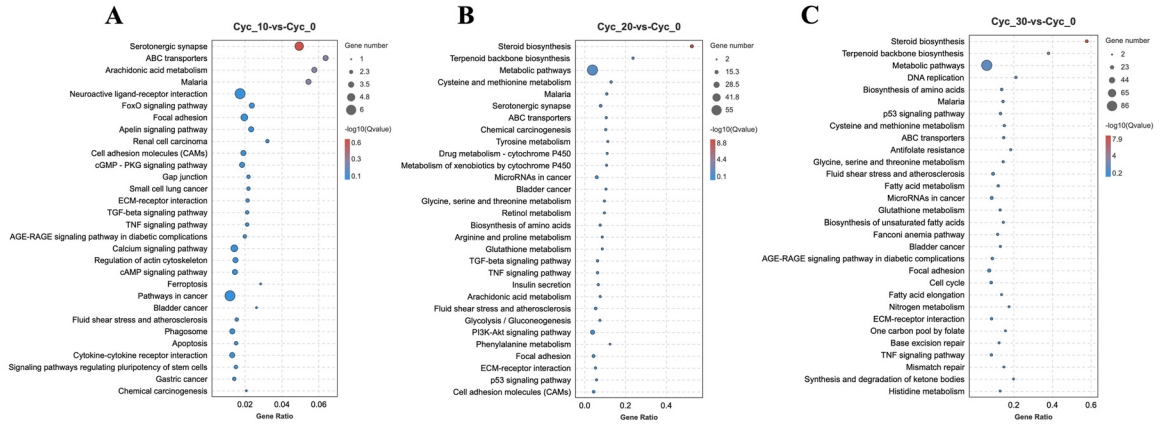

Figure 3. KEGG pathway analysis. (A-C) KEGG pathway analysis of DEGs in Cyc_10 (A), Cyc_20 (B), and Cyc_30 (C). X-axis: number of differential genes enriched in the current pathway/number of species enriched in the current pathway. Y-axis: different pathways. The size of the bubble indicated the number of genes enriched in current pathway.

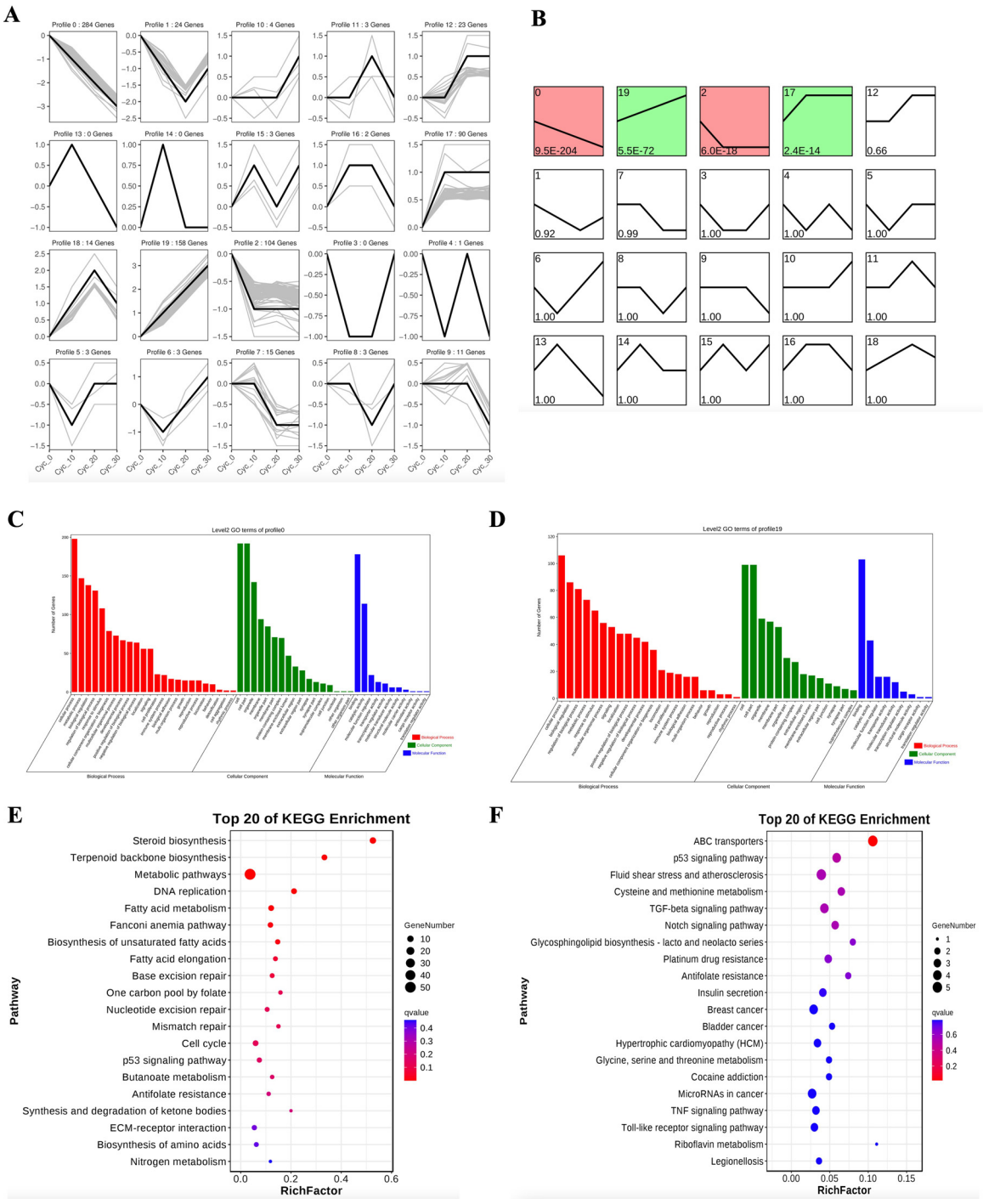

Figure 4. Gene expression pattern analysis. (A) General chart of all gene expression trend profiles. (B) Gene expression trend profiles are ordered based on the *P*-value significance of the number of genes assigned versus expected. Red: significantly clustered in downtrend genes profiles. Green: significantly clustered in uptrend genes profiles. (C and D) GO functional enrichment analysis of DEGs in profile 0 (C) and profile 19 (D). (E and F) KEGG pathway analysis of DEGs in profile 0 (E) and profile 19 (F).

transcriptome results suggest that cycloleucine could regulate muscle cell proliferation, so we detected the effect of cycloleucine in myoblast cells. The mRNA level of cell cycle related genes *CCNB1, CDK1*, and *CDK2* were depressed (Figure 5C) and cells in the S phase were significantly decreased after cycloleucine treatment (Figure 5D). Cycloleucine could significantly reduce the number of myoblast cells in proliferative stage as shown in CCK-8 assay results (Figure 5E) and EdU staining (Figure 5F-G).

Cycloleucine Inhibits Myoblast Cells Differentiation

As shown in Figure 3A that cycloleucine could negatively regulate skeletal muscle cell differentiation, so we detected the mRNA level of some myogenesis marker genes like *MyoD, c-Myc, Myomarker, and Myf5.* The expression of *MyoD* were consistently decreased as the cycloleucine concentration increased (Figure 6A), the expression of *c-Myc* and *Myomarker* were also

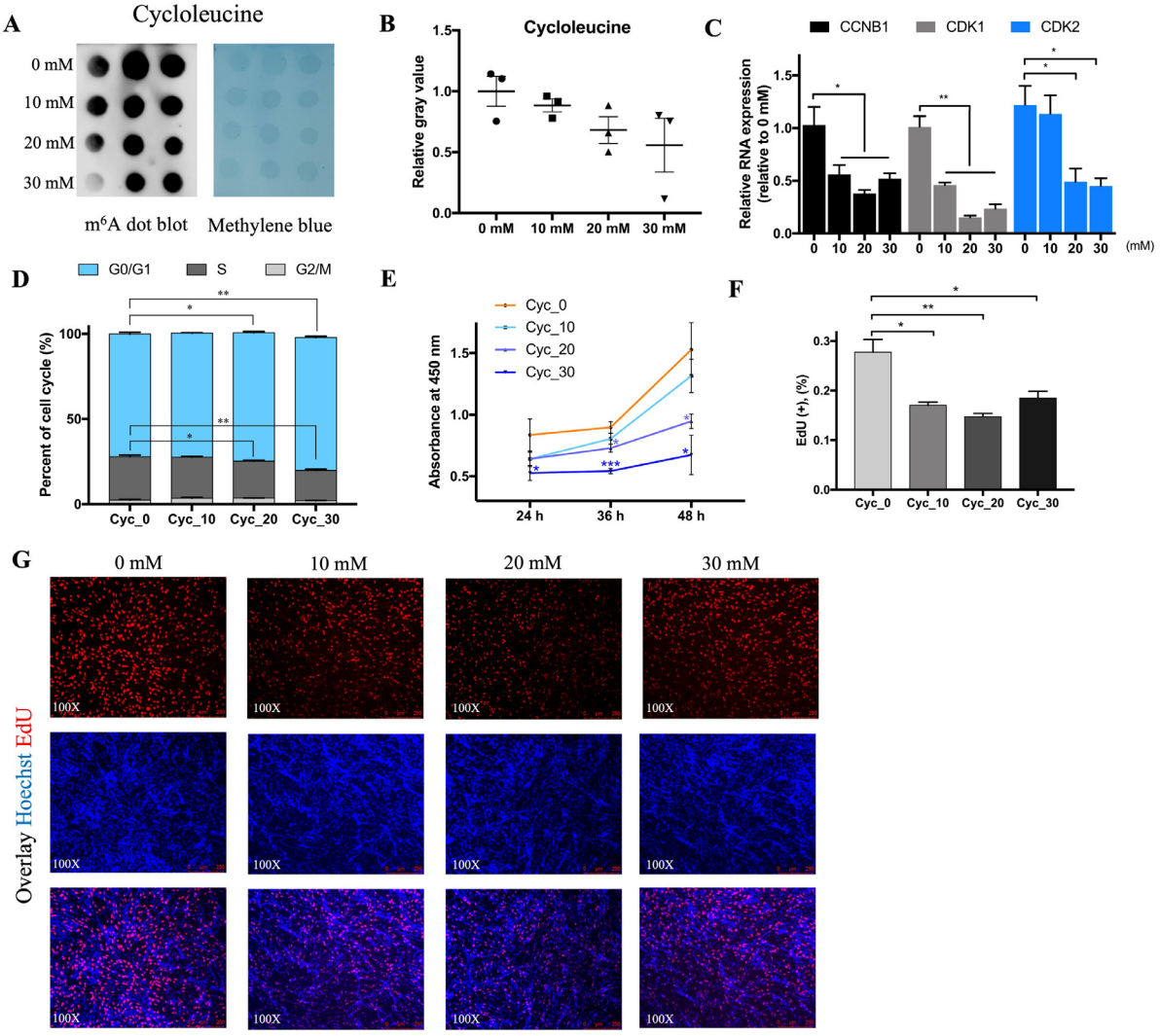

Figure 5. Cycloleucine decreases the m^{6}A level and depresses myoblast cell proliferation. (A) RNA dot blot was used to detect the m^{6}A modification after being treated with 0, 10, 20, and 30 mM cycloleucine for 24 h, methylene blue staining was used as a loading control (n = 3). (B) The relative gray value of RNA dot blot. (C) qRT-PCR results for *CCNB1, CDK1*, and *CDK2* after treated with 0, 10, 20, and 30 mM cycloleucine for 24 h. (D) Distribution proportion of different cell stages after 24 h cycloleucine treatment. (E) The statistical results of CCK-8 assay after 24 h, 36 h, and 48 h cycloleucine treatment. (F and G) The EdU positive cell rate (F) and EdU staining (G) of myoblast cells being treated with cycloleucine. (*$P < 0.05$, **$P < 0.01$)

significantly decreased after cycloleucine treatment (Figure 6A). In the meantime, the western blot result showed that MyHC could be inhibited (Figure 6B), and when we treated the myoblasts induced for differentiation on day 2 with cycloleucine for 24 h, with the increased concentration, the differentiation process, as well as the myotube area was significantly inhibited (Figure 6C, D).

DISCUSSION

Recently m^{6}A has been proved to be important in many biogenesis. Cycloleucine, an inhibitor of nucleic acid methylation, is a good material to study m^{6}A level in myogenesis. When RNA methylation level of muscle cells is inhibited by different concentration of cycloleucine, the dynamic change of related RNA were easily captured by RNA Sequencing. Previous research showed 40 mM of cycloleucine blocks the formation of m^{6}A by greater than 90% after 24 h (Dimock and Stolzfus, 1978), while another one did a concentration gradient at 0, 1, 5, 10 mM cycloleucine to treat C2C12 cells for 24 h and found cycloleucine could decrease m^{6}A level in a dose-dependent manner and 10 mM of cycloleucine could decrease m^{6}A level through all C2C12 cell differentiation stage (Chen et al., 2019). So here in our study, we chose 0, 10, 20, 30 mM cycloleucine to treat chicken primary myoblasts and found the inhibition of cycloleucine on the m^{6}A level of chicken myoblast cells was continuously reducing (Figure 5A), basically consistent with the above research but the inhibition of 30 mM cycloleucine in m^{6}A level was about 50% after 24 h, which means the decreased m^{6}A level could inhibit myogenesis.

In this study, the number of DEGs were increased with the rise of cycloleucine concentration and these DEGs mainly showed four expression patterns, of which about 59% showed concentration dependence (profile 0 and 19), their expression level either increased or decreased continuously, however, the promotion of inhibition of cycloleucine on the expression of another part of genes (profile 2 and 17) does not change with the increased of

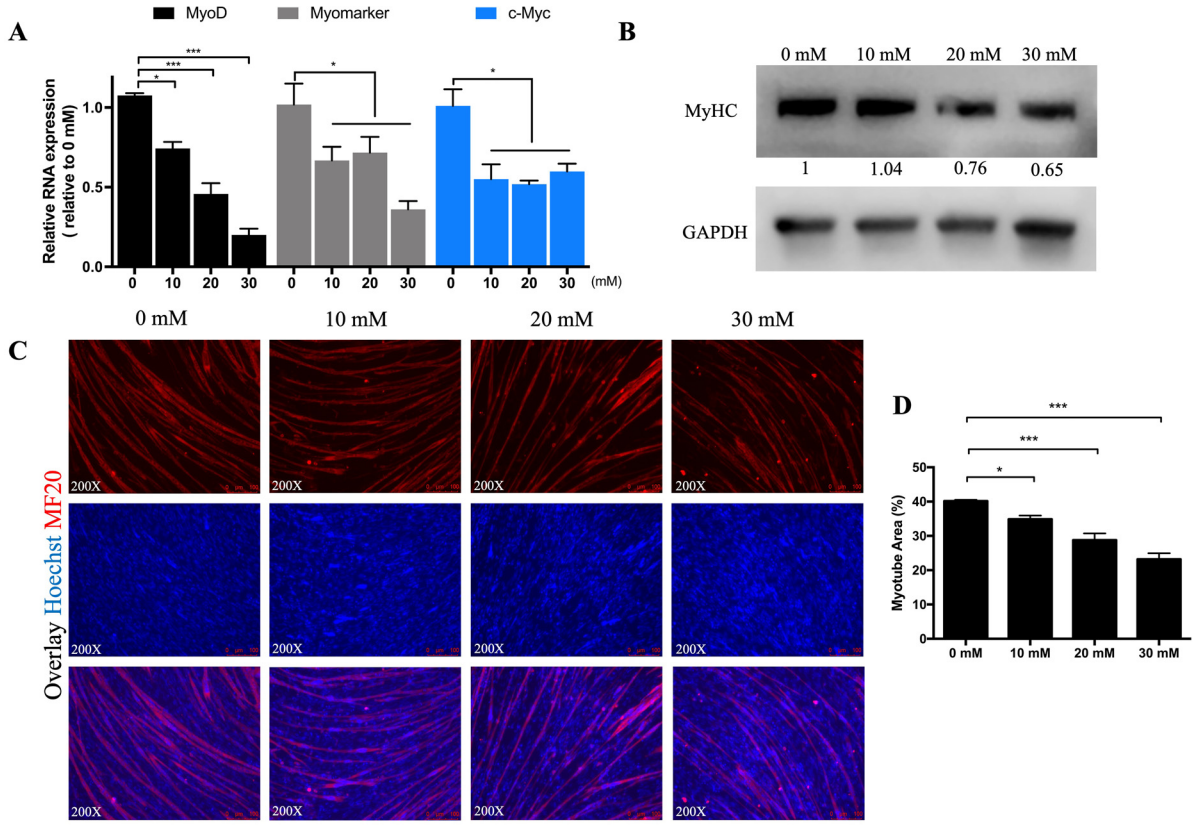

Figure 6. Cycloleucine inhibit myotube formation. (A) qRT-PCR results for *MyoD, c-Myc*, and *Myomarker* after treatment with 0, 10, 20, and 30 mM cycloleucine for 24 h. (B) The protein expression of MyHC determined by Western blotting. (C and D) MF20 immunofluorescence staining (C) and myotube area (%) analysis (D) of MF20 immunofluorescence staining after being treated with 0, 10, 20, and 30 mM cycloleucine for 24 h at D2. ($*P < 0.05$, $***P < 0.001$)

concentration. Also, with the raised concentration, GO functional enrichment analysis shifts from the skeletal muscle cell proliferation and differentiation to specific metabolic and biosynthetic processes indicates as a non-metabolizable amino acid, cycloleucine can still participate in the synthesis and metabolism of some molecules, thus playing an inhibitory role in myogenesis.

Research has found that the limitation of S-adenosyl methionine could trigger cell cycle arrest in G1 (Lin et al., 2014), which we consistently found here in this study that cycloleucine, an inhibitor of methionine adenosyl transferase and reducer of S-adenosyl methionine level (Lombardini and Talalay, 1970b), could inhibit cell cycle progress by stopping S phase initiation and accumulation cells in G0/G1 phase (Figure 5D). Since CDK1 and CDK2 are responsible for the S phase of cell cycle (Schafer, 1998), low activity of CDK1 and CDK2 could induce lower DNA synthesis thus leading to G1 arrest. Unlike what they found in murine myoblasts that 10 mM cycloleucine could inhibit the expression of *MyoD, MyoG, Myf5*, and *Myf6* (Chen et al., 2019), the expression pattern of those genes in this study were not the same, maybe due to the species difference or because the cells we used for mRNA-Seq were in the proliferative phase. Despite the EdU positive cells not constantly decreasing with the increase of concentration, the myogenesis process was inhibited in a dose-dependent manner.

Commonly, MyoD and Myf5 are participated in myoblast determination, whereas MyoG is involved in the late differentiation stage (Sartorelli and Caretti, 2005; Ferri et al., 2009). Research showed that the m^6A modification of *MyoD* is essential for *MyoD* mRNA expression in proliferative myoblasts (Kudou et al., 2017), which is consistent with our results that with a decreased m^6A level, the expression of *MyoD* was also decreased (Figures 5A, and 6A), suggesting the RNA stability of *MyoD* was destroyed with the occurrence of RNA demethylation. MyHC (myosin heavy chain) is a skeletal muscle specific contractile protein expressed during myogenesis and muscle development (Acakpo-Satchivi et al., 1997), the loss of MyHC could lead to low fusion index and myogenic differentiation defects (Agarwal et al., 2020). Our result in Figure 6B to D proved that cycloleucine could inhibit the differentiation of myoblasts by inhibiting MyHC expression and myotube formation.

In conclusion, cycloleucine could continuously reduce the m^6A level of myoblast cells and inhibit myogenesis by depressing myoblast cell proliferation and myotube formation.

ACKNOWLEDGMENTS

This research was carried out with the support of the Natural Scientific Foundation of China (U1901206), Local Innovative and Research Teams Project of Guangdong Province (2019BT02N630), the Science and Technology Program of Guangdong province, China

(2020B1212060060), the Science and Technology Program of Guangzhou, China (202103000084), the Construction Project of Modern Agricultural Science and Technology Innovation Alliance in Guangdong Province (2021KJ128), National Key R&D Program of China (2021YFD1300100), and China Agriculture Research System (CARS-41-G03).

DISCLOSURES

All authors agree and declare that they have no competing interests.

SUPPLEMENTARY MATERIALS

Supplementary material associated with this article can be found in the online version at doi:10.1016/j.psj.2022.102219.

REFERENCES

Acakpo-Satchivi, L. J., W. Edelmann, C. Sartorius, B. D. Lu, P. A. Wahr, S. C. Watkins, J. M. Metzger, L. Leinwand, and R. Kucherlapati. 1997. Growth and muscle defects in mice lacking adult myosin heavy chain genes. J. Cell Biol. 139:1219–1229.

Agarwal, M., A. Sharma, P. Kumar, A. Kumar, A. Bharadwaj, M. Saini, G. Kardon, and S. J. Mathew. 2020. Myosin heavy chain-embryonic regulates skeletal muscle differentiation during mammalian development. Development 147:dev184507.

Amor, S., and H. E. Webb. 1987. The effect of cycloleucine on SFV A7 (74) infection in mice. Br. J. Exp. Pathol. 68:225–235.

Bentzinger, C. F., Y. X. Wang, and M. A. Rudnicki. 2012. Building muscle: molecular regulation of myogenesis. Cold Spring Harb. Perspect Biol 4:a008342.

Caboche, M., and J. P. Bachellerie. 1977. RNA methylation and control of eukaryotic RNA biosynthesis. Effects of cycloleucine, a specific inhibitor of methylation, on ribosomal RNA maturation. Eur. J. Biochem. 74:19–29.

Chen, J. N., Y. Chen, Y. Y. Wei, M. A. Raza, Q. Zou, X. Y. Xi, L. Zhu, G. Q. Tang, Y. Z. Jiang, and X. W. Li. 2019. Regulation of m^(6)A RNA methylation and its effect on myogenic differentiation in murine myoblasts. Mol. Biol. (Mosk). 53:436–445.

Coulter, A. W., J. B. Lombardini, and P. Talalay. 1974. Structural and conformational analogues of L-methionine as inhibitors of the enzymatic synthesis of S-adenosyl-L-methionine. II. Aromatic amino acids. Mol. Pharmacol. 10:305–314.

Dimock, K., and C. M. Stolzfus. 1978. Cycloleucine blocks 5′-terminal and internal methylations of avian sarcoma virus genome RNA. Biochemistry. 17:3627–3632.

Ernst, J., and Z. Bar-Joseph. 2006. STEM: a tool for the analysis of short time series gene expression data. BMC Bioinformatics 7:191.

Feng, Y., J. H. Cao, X. Y. Li, and S. H. Zhao. 2011. Inhibition of miR-214 expression represses proliferation and differentiation of C2C12 my-oblasts. Cell Biochem. Funct. 29:378–383.

Ferri, P., E. Barbieri, S. Burattini, M. Guescini, A. D'Emilio, L. Biagiotti, P. D. Grande, A. D. Luca, V. Stocchi, and E. Falcieri. 2009. Expression and subcellular localization of myogenic regulatory factors during the differentiation of skeletal muscle C2C12 myoblasts. J. Cell Biochem. 108:1302–1317.

Fu, Y., D. Dominissini, G. Rechavi, and C. He. 2014. Gene expression regulation mediated through reversible m^{6}A RNA methylation. Nat. Rev. Genet. 15:293–306.

Fustin, J. M., M. Doi, Y. Yamaguchi, H. Hida, S. Nishimura, M. Yoshida, T. Isagawa, M. S. Morioka, H. Kakeya, I. Manabe, and H. Okamura. 2013. RNA-methylation-dependent RNA processing controls the speed of the circadian clock. Cell. 155:793–806.

Gheller, B. J., J. E. Blum, E. H. H. Fong, O. V. Malysheva, B. D. Cosgrove, and A. E. Thalacker-Mercer. 2020. A defined N6-methyladenosine (m6A) profile conferred by METTL3 regulates muscle stem cell/myoblast state transitions. Cell Death Discov. 6:95.

Glickman, M. E., S. R. Rao, and M. R. Schultz. 2014. False discovery rate control is a recommended alternative to Bonferroni-type adjustments in health studies. J. Clin. Epidemiol. 67:850–857.

Jia, G., Y. Fu, X. Zhao, Q. Dai, G. Zheng, Y. Yang, C. Yi, T. Lindahl, T. Pan, Y. G. Yang, and C. He. 2011. N6-methyladenosine in nuclear RNA is a major substrate of the obesity-associated FTO. Nat. Chem. Biol. 7:885–887.

Kudou, K., T. Komatsu, J. Nogami, K. Maehara, A. Harada, H. Saeki, E. Oki, Y. Maehara, and Y. Ohkawa. 2017. The requirement of Mettl3-promoted MyoD mRNA maintenance in proliferative myoblasts for skeletal muscle differentiation. Open Biol. 7:170119.

Lee, M., B. Kim, and V. N. Kim. 2014. Emerging roles of RNA modification: m(6)A and U-tail. Cell. 158:980–987.

Li, J., Y. Pei, R. Zhou, Z. Tang, and Y. Yang. 2021. Regulation of RNA N6-methyladenosine modification and its emerging roles in skeletal muscle development. Int. J. Biol. Sci. 17:1682–1692.

Lin, D. W., B. P. Chung, and P. Kaiser. 2014. S-adenosylmethionine limitation induces p38 mitogen-activated protein kinase and triggers cell cycle arrest in G1. J. Cell Sci. 127(Pt 1):50–59.

Livak, K. J., and T. D. Schmittgen. 2001. Analysis of relative gene expression data using real-time quantitative PCR and the 2(-Delta C(T)) Method. Methods. 25:402–408.

Lombardini, J. B., A. W. Coulter, and P. Talalay. 1970a. Analogues of methionine as substrates and inhibitors of the methionine adenosyltransferase reaction. Deductions concerning the conformation of methionine. Mol. Pharmacol. 6:481–499.

Lombardini, J. B., and P. Talalay. 1970b. Formation, functions and regulatory importance of S-adenosyl-L-methionine. Adv. Enzyme Regul. 9:349–384.

Luo, W., J. Chen, L. Li, X. Ren, T. Cheng, S. Lu, R. A. Lawal, Q. Nie, X. Zhang, and O. Hanotte. 2019. c-Myc inhibits myoblast differentiation and promotes myoblast proliferation and muscle fibre hypertrophy by regulating the expression of its target genes, miRNAs and lincRNAs. Cell Death Differ. 26:426–442.

Luo, W., Q. Nie, and X. Zhang. 2013. MicroRNAs involved in skeletal muscle differentiation. J. Genet. Genomics. 40:107–116.

Millay, D. P., J. R. O'Rourke, L. B. Sutherland, S. Bezprozvannaya, J. M. Shelton, R. Bassel-Duby, and E. N. Olson. 2013. Myomaker is a membrane activator of myoblast fusion and muscle formation. Nature. 499:301–305.

Sartorelli, V., and G. Caretti. 2005. Mechanisms underlying the transcriptional regulation of skeletal myogenesis. Curr. Opin. Genet. Dev. 15:528–535.

Schafer, K. A. 1998. The cell cycle: a review. Vet. Pathol. 35:461–478.

Schwartz, S., S. D. Agarwala, M. R. Mumbach, M. Jovanovic, P. Mertins, A. Shishkin, Y. Tabach, T. S. Mikkelsen, R. Satija, G. Ruvkun, S. A. Carr, E. S. Lander, G. R. Fink, and A. Regev. 2013. High-resolution mapping reveals a conserved, widespread, dynamic mRNA methylation program in yeast meiosis. Cell. 155:1409–1421.

Tajbakhsh, S. 2009. Skeletal muscle stem cells in developmental versus regenerative myogenesis. J. Intern. Med. 266:372–389.

Wang, X., N. Huang, M. Yang, D. Wei, H. Tai, X. Han, H. Gong, J. Zhou, J. Qin, X. Wei, H. Chen, T. Fang, and H. Xiao. 2017. FTO is required for myogenesis by positively regulating mTOR-PGC-1α pathway-mediated mitochondria biogenesis. Cell Death Dis. 8:e2702.

Wang, Y., Y. Li, J. I. Toth, M. D. Petroski, Z. Zhang, and J. C. Zhao. 2014. N6-methyladenosine modification destabilizes developmental regu-lators in embryonic stem cells. Nat. Cell Biol. 16:191–198.

Zhang, X., Y. Yao, J. Han, Y. Yang, Y. Chen, Z. Tang, and F. Gao. 2020. Longitudinal epitranscriptome profiling reveals the crucial role of N6-methyladenosine methylation in porcine prenatal skeletal muscle development. J. Genet. Genomics. 47:466–476.

Zheng, G., J. A. Dahl, Y. Niu, P. Fedorcsak, C. M. Huang, C. J. Li, C. B. Vågbø, Y. Shi, W. L. Wang, S. H. Song, Z. Lu, R. P. Bosmans, Q. Dai, Y. J. Hao, X. Yang, W. M. Zhao, W. M. Tong, X. J. Wang, F. Bogdan, K. Furu, Y. Fu, G. Jia, X. Zhao, J. Liu, H. E. Krokan, A. Klungland, and Y. G. Yang. 2013. ALKBH5 is a mammalian RNA demethylase that impacts RNA metabolism and mouse fertility. Mol. Cell 49:18–29.